

High efficiency nanocomposite sorbents for CO₂ capture based on amine-functionalized mesoporous capsules†

Genggeng Qi,^a Yanbing Wang,^a Luis Estevez,^a Xiaonan Duan,^a Nkechi Anako,^b Ah-Hyung Alissa Park,^b Wen Li,^c Christopher W. Jones^c and Emmanuel P. Giannelis^{*a}

Received 2nd July 2010, Accepted 10th September 2010

DOI: 10.1039/c0ee00213e

A novel high efficiency nanocomposite sorbent for CO₂ capture has been developed based on oligomeric amine (polyethylenimine, PEI, and tetraethylenepentamine, TEPA) functionalized mesoporous silica capsules. The newly synthesized sorbents exhibit extraordinary capture capacity up to 7.9 mmol g⁻¹ under simulated flue gas conditions (pre-humidified 10% CO₂). The CO₂ capture kinetics were found to be fast and reached 90% of the total capacities within the first few minutes. The effects of the mesoporous capsule features such as particle size and shell thickness on CO₂ capture capacity were investigated. Larger particle size, higher interior void volume and thinner mesoporous shell thickness all improved the CO₂ capacity of the sorbents. PEI impregnated sorbents showed good reversibility and stability during cyclic adsorption–regeneration tests (50 cycles).

Introduction

Carbon dioxide has drawn significant attention as one of the main anthropogenic contributors to climate change.¹ A wide range of approaches, including solvents,^{2–5} cryogenic techniques,⁶ membranes,^{7,8} and solid sorbents,^{9–11} have been proposed to capture CO₂. Among these approaches, amine scrubbing is the current state-of-the-art technology for CO₂ capture on industrial scale.¹² Although amines, in particular aqueous solutions of monoethanolamine (MEA), are effective at capturing CO₂, they suffer from several disadvantages. They are corrosive and, therefore, increase construction cost. In addition, they do gradually volatilize and degrade, especially in the presence of oxygen and/or sulfur dioxide, both of which necessitate the periodic injection of fresh solution. Furthermore, when MEA

is applied to flue gas purification in conventional absorber/stripper systems in power plants, the parasitic energy consumption required for regeneration is considerable (up to 30%). The combined costs of CO₂ capture and compression raise the price of generating electrical power by over 60%. Reducing that percentage is a primary goal of R&D activity, much of which has been exploring the performance of alternative sorbents including amines other than MEA.¹³

Porous solids such as zeolites or activated carbon are good candidates for capturing CO₂ from flue gas through physical adsorption.¹⁴ High porosities endow activated carbon and zeolites with CO₂ capture capacities of 2–3.5 mmol g⁻¹. However, the CO₂/N₂ selectivity of activated carbon is relatively low (~10), which makes carbon-based systems practical only for CO₂-rich flue gas.¹⁵ Although zeolites offer better CO₂/N₂ selectivities than those of carbonaceous materials, their CO₂ capacities degrade significantly, when water vapor is present in the flue gas.¹⁴

CO₂ capture by solid sorbents based on amines immobilized in porous solids has been an increasingly active area of research.¹⁴ A variety of amines, supports and immobilizing techniques have been tested and the results have been quite promising.^{11,16,17} In contrast to amine scrubbers, solid-supported amine sorbents offer significant advantages for CO₂ capture, including potential elimination of corrosion problems and lower energy cost for sorbent regeneration. Solid-supported amine sorbents exhibit

^aDepartment of Materials Science and Engineering, Cornell University, Ithaca, NY, 14853, USA. E-mail: epg2@cornell.edu

^bDepartment of Earth and Environmental Engineering and Department of Chemical Engineering, Columbia University, New York, NY, 10027, USA

^cSchool of Chemical & Biomolecular Engineering, Georgia Institute of Technology, 311 Ferst Drive, Atlanta, GA, 30332, USA

† Electronic supplementary information (ESI) available: Adsorption isotherms of MC400/10 and MC400/10PEI%75 composite sorbent and viscosity difference of amines before and after CO₂ capture. See DOI: 10.1039/c0ee00213e

Broader context

Increases in atmospheric carbon dioxide gas have been linked to increasing use of fossil fuels over the past century. Post-combustion capture has the greatest near-term potential for reducing CO₂ emissions. Solid sorbents provide a promising alternative to conventional amine solutions for CO₂ capture. However, practical CO₂ capture applications have been impeded primarily by limited sorbent capacity and recyclability. Here we present a novel CO₂ capture platform based on oligomeric amines supported on specially engineered mesoporous hollow particles (mesoporous capsules). This new design leads to an exceptional capture capacity of up to 7.9 mmol g⁻¹ under simulated flue gas conditions outperforming both conventional monoethanolamine solutions and other current solid amine impregnated sorbents. In addition to their outstanding CO₂ capture capacity, the sorbents are readily regenerated at relatively low temperature and exhibit good stability and recyclability.

high selectivity and reversibility for CO₂ capture due to the specific CO₂-amine chemistry. Unlike zeolites and activated carbon, amine-functionalized sorbents have been proved to be tolerant, and even positive to moisture during CO₂ capture, thus eliminating the need for strict humidity control prior to CO₂ capture.^{18,19}

Because of their numerous advantages, intensive efforts have been directed towards the development of solid-supported amine sorbents. Essentially, two strategies have been used: covalently tethered or physically impregnated amines to solid supports with large surface area such as mesoporous materials.^{9,11,17,20–28} Jones *et al.* developed a hyperbranched aminosilicate material by a one-step reaction between aziridine and SBA-15, and achieved a capacity about 3.1 mmol g⁻¹ at 25 °C in simulated flue gas conditions.¹¹ The material showed a capacity up to 5.5 mmol g⁻¹ at 25 °C and 4.2 mmol g⁻¹ at 75 °C with higher amine grafting.²⁹ Song *et al.* reported the first polyethylenimine impregnated MCM-41 sorbent with a capacity around 3 mmol g⁻¹ at 75 °C in 1 atm dried CO₂. The capacity was further improved to 3.2 mmol g⁻¹ using SBA-15 as support in simulated flue gas conditions.^{9,28} As-synthesized MCM-41 particles were also tested as support for tetraethylenepentamine and a high CO₂ capacity of up to 5.4 mmol g⁻¹ was obtained at 75 °C in 1 atm dried CO₂. However, this sorbent showed limited recyclability.²³

Although solid-supported amine sorbents provide a promising alternative for CO₂ capture, high capture efficiency with good recyclability are required in order to develop an economically feasible industrial-scale process. Schuette *et al.* have evaluated recently post-combustion CO₂ capture options based on a plant producing 1060 ton CO₂ per day.³⁰ They compared the cost of capturing 90% CO₂ using 20% MEA solution vs. a solid sorbent based on polyethylenimine impregnated mesoporous silica. According to their calculations, if the CO₂ capture capacity is less than 3 mmol g⁻¹ the economics will favor MEA. However, the solid sorbent starts becoming more favorable compared to MEA as the capture capacity increases to more than 4 mmol g⁻¹.

Almost all of the work to date has been focused on the immobilization of amines on as-synthesized or calcined mesoporous materials. Further improvement of the CO₂ capture capacity of the sorbents has become challenging because of limitations with the amount of amine loaded and the availability of active sites for CO₂ capture in the sorbents. To overcome these limitations, we have been focusing on the development of a novel CO₂ capture platform based on oligomeric amines supported on specially engineered mesoporous hollow particles (mesoporous capsules).³¹ This new design greatly enhances amine incorporation and facilitates transport of CO₂ inside the sorbent leading to exceptional capture capacity of 6.6 mmol g⁻¹ under 1 atm dried CO₂ gas at 75 °C. This capacity represents an improvement of at least 400 and 25% over that of conventional monoethanolamine solution (15% MEA) and other current solid amine impregnated sorbents, respectively, under similar CO₂ capture conditions. More importantly the composite sorbents show an extraordinary capacity up to 7.9 mmol g⁻¹ at 75 °C under simulated flue gas conditions (pre-humidified 10% CO₂). In addition to their outstanding CO₂ capture capacity, the sorbents are readily regenerated at relatively low temperature (<100 °C) and exhibit good stability over repetitive adsorption-desorption cycling (50 cycles).

Experimental

All chemicals were purchased from Aldrich unless otherwise stated. 2,2'-Azobis(2-methylpropionamide) dihydrochloride (V-50, >97.0%), polyvinylpyrrolidone (K-30, >99.5%), hexadecyltrimethylammonium bromide (CTAB, >99.0%), [2-(acryloyloxy)ethyl] trimethylammonium chloride (AETAC, 80 wt% in water), ammonium hydroxide solution (~30.0%), glycerol diglycidyl ether (GDE), ethylenimine oligomer mixture (PEI, average $M_n \approx 423$), and tetraethylenepentamine (TEPA) were used without further purification. Styrene (St, >99.0%) was washed through an inhibitor remover column to remove *tert*-butylcatechol and then distilled under reduced pressure prior to use. Tetraethoxysilane (TEOS, >99.9%, Gelest) and ethanol (80%, VWR) were used as received. Deionized water was generated with a Milli-Q integral pure and ultrapure water purification system.

Synthesis of mesoporous silica supports

Mesoporous silica capsules with different sizes and shell thickness, denoted as MC x / y , where x and y represent the approximate diameter and the shell thickness of the mesoporous capsules in nanometres, respectively, were prepared as we described previously.³¹ Briefly, for MC160/20, CTAB (0.8 g) was dissolved in a mixture of water (29.0 g), ethanol (12.0 g) and ammonium hydroxide solution (1.0 ml). Polystyrene latex with an average size around 130 nm (9.3 wt%, 10.0 g) was added dropwise to the above CTAB solution at room temperature under vigorous stirring, followed by sonication for 10 min. The derived milky mixture was then magnetically stirred for 30 min before adding dropwise TEOS (4.0 g). The molar ratio of TEOS/CTAB/ethanol/H₂O/NH₃ was 1.0 : 0.11 : 13 : 87 : 0.83, and the TEOS/polystyrene weight ratio was 4.3. The mixture was kept at room temperature for 48 h before the mesoporous silica coated latex was harvested by centrifugation at 7000 rpm for 40 min. The precipitate was washed with copious amounts of ethanol and then dried at room temperature. Finally the material was calcined in air at 600 °C for 8 h using a heating rate at 3 °C min⁻¹. For MC400/20, polystyrene latex with an average size around 400 nm (9.3 wt%, 25 g) was added dropwise to a mixture of CTAB (0.80 g), water (9.6 g), ethanol (11.0 g) and ammonium hydroxide solution (2.0 ml) under vigorous stirring. The derived mixture was sonicated for 10 min and then magnetically stirred for 30 min before adding dropwise TEOS (1.5 g). The TEOS/CTAB/ethanol/H₂O/NH₃ molar ratio was 1 : 0.30 : 32 : 88 : 4.4, and the TEOS/polystyrene weight ratio was 0.66. The mixture was kept at room temperature for 48 h before the mesoporous silica coated latex was recovered by centrifugation at 7000 rpm for 15 min, followed by copious washings with ethanol. The precipitate was dried in the air overnight and calcined at 600 °C for 8 h in air. MC400/10 and MC400/50 were prepared in the same manner as MC400/20 except that 0.75 g and 3.0 g of TEOS were used, respectively.

To investigate the effect of the support on the capacity of the sorbents, three other supports were synthesized. Silica coated polystyrene nonporous solid nanoparticles with a diameter around 400 nm, SiO₂-400, were synthesized in the same manner as MC400/10 but without adding CTAB. The derived SiO₂-400

nanoparticles were washed with ethanol and dried in air at room temperature. Normal, non-hollow MCM-41 mesoporous particles were prepared similarly to MC400/10 except no polystyrene latex was used. Mesoporous SBA-15 particles were synthesized as described previously.³²

Synthesis of amine-functionalized sorbents

The nanocomposite sorbents were prepared *via* wet impregnation. In a typical preparation, a given amount of PEI or TEPA in ethanol (10 wt%) was added to 50 mg of mesoporous capsules or other supports. The resultant mixture was continuously stirred for about 30 min and then dried at 40 °C for 24 h under reduced pressure (700 mmHg). The thus formed sorbents are denoted as MC x /yPEI% z , where x and y represent the diameter and the shell thickness of the mesoporous capsules in nanometres, respectively, and z the weight percentage of amine in the sorbent.

CO₂ capture and regeneration of sorbents

CO₂ adsorption/desorption measurements under dry conditions were performed on a TA Instruments Q5000 thermal graphic analyzer. Dried pure CO₂ (99.99%) or CO₂ (19.98%) balanced with N₂ at 1 atm was used for the adsorption runs and ultra high purity N₂ (99.995%) was used as a purging gas for CO₂ desorption. In a typical adsorption process, about 10 mg of the sorbent were placed in a platinum sample pan. After the sorbent was heated to 100 °C in a N₂ stream (25 ml min⁻¹) for 60 min to remove all the moisture and CO₂ adsorbed from the air, the temperature was decreased to 75 °C at a rate of 20 °C min⁻¹. The gas was then switched from N₂ to CO₂ (25 ml min⁻¹) and the sorbent was kept at 75 °C for 120 min for the adsorption study. The CO₂ capturing capacity of the sorbent in mmol g⁻¹ was calculated from the weight gain of the sample in the adsorption process.

CO₂ adsorption/desorption in simulated flue gas was measured with a packed bed flow reactor with an online mass spectrometer as described previously.^{11,29} Approximately 70 mg of adsorbent were dispersed in 300 mg of sieved sand (250 to 425 μm) and loaded into a Pyrex tubular reactor (1/4 in. outer diameter). 10% CO₂ balanced with Ar was pre-humidified to a steady state by flowing through two glass water bubblers at room temperature. After the samples were completely purged with dry Ar for 1 h at 110 °C, the reactor was switched to the test gas at a flow rate of about 20 ml min⁻¹. Adsorption was then performed for 1 h at 75 °C. The CO₂ concentration at the reactor outlet was measured with a Pfeiffer Vacuum QMS 200 Prisma Quadrupole Mass Spectrometer (MS). The CO₂ breakthrough plot is shown in Fig. S1†. The amount of CO₂ adsorbed was calculated from the MS output as reported before.^{11,29}

Two different methods, temperature swing and concentration sweep (altered CO₂ partial pressure in adsorption and desorption), were used for CO₂ desorption. In the temperature swing the sorbent was first exposed to CO₂ at 75 °C for 10 min. The gas was then switched from CO₂ to pure N₂ (25 ml min⁻¹) and the temperature was increased to 100 °C at a rate of 20 °C min⁻¹ and held at that temperature for 10 min to regenerate the sorbent. For the concentration sweep the gas was switched to pure N₂ (25

ml min⁻¹) at 75 °C after 10 min CO₂ adsorption. The sorbent was then kept at 75 °C in N₂ for 25 min for sorbent regeneration.

Characterization

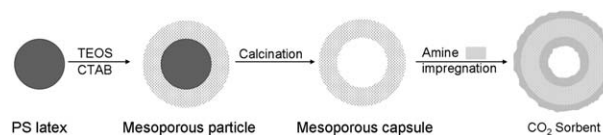
Bright-field TEM images were obtained by a FEI Tecnai T12 Spirit Twin TEM/STEM operated at 120 kV. Samples were prepared by dispersing the material in ethanol using sonication. A few drops of the dispersion were loaded onto a carbon coated copper microgrid and dried in air. To investigate the morphology of amine impregnated sorbents, a given amount of polyethylenimine and glycerol diglycidyl ether (v/v = 1 : 1) ethanol solution (21.4 wt%) was impregnated into the silica supports. These composites were dried at 20 °C for 24 h under reduced pressure (700 mmHg) and then cured at 80 °C for 6 h. The derived composites using MC400/10, MCM-41 and SBA-15 are denoted as MC400/10PEI-GDE% m , MCM-41PEI-GDE% m and SBA-15PEI-GDE% m , respectively, where m is the polymer loading equivalent to z in pure amine impregnated capsules MC x /yPEI% z . Since MCM-41PEI-GDE%83 and SBA-15PEI-GDE%83 are gels, they were cut by a Leica UC7 cryomicrotome into 100 nm slices at -60 °C and loaded onto carbon coated copper microgrids *via* dry pickup. For MC400/10PEI-GDE%83, a small amount of the powder was carefully adhered onto quick-drying glue and then cut under the same conditions as MCM-41PEI-GDE%83 and SBA-15PEI-GDE%83 for TEM specimen preparation.

XRD patterns of the mesoporous materials were obtained on a Scintag diffractometer using CuK α ($\lambda = 1.54 \text{ \AA}$) radiation. FT-IR spectra of the samples were recorded on a Nicolet Smart iTR™ iZ10 spectrometer. Nitrogen adsorption-desorption isotherms were obtained on a Quantachrome Nova 3000 BET specific surface area analyzer at liquid nitrogen temperature. The specific surface areas of the samples were calculated by the Brunauer-Emmett-Teller (BET) method. The pore size distributions were calculated from the adsorption isotherm using the Barrett-Joyner-Halenda (BJH) model.

Results and discussion

Design and characterization of CO₂ sorbents

The new sorbents are based on polyethylenimine, PEI, and tetraethylenepentamine, TEPA, supported on specially designed mesoporous SiO₂ hollow capsules. The silica capsules are readily prepared from TEOS in the presence of a polystyrene latex template (Scheme 1). A mesoporous shell with tunable thickness is grown around the polystyrene particles with the assistance of CTAB acting as mesopore directing agent. After synthesis the templates are removed by calcination to yield a capsule with a mesoporous SiO₂ shell.³¹



Scheme 1 Synthesis of amine impregnated composite sorbents based on mesoporous capsules.

The structure of the support plays an important role in the performance of the new sorbents. The main requirement for developing more efficient amine-functionalized CO₂ sorbents is the use of a support with well-defined structure, in particular high surface area and pore volume, as well as proper pore size. Simple porous materials such as amorphous SiO₂ gel with random pore sizes and shapes are poor candidates, since only a limited amount of the pore area and pore volume can be accessible.^{33,34} Mesoporous silica with pore diameters in the nanometre range greatly increases the accessible sorption sites on/in the sorbent and improves the mass transfer during the sorption/desorption process. Unfortunately, not all the pores are available for CO₂ capture. When a large amount of amines is loaded, the pore channels are significantly constricted and even blocked. In addition, the amino groups may be unevenly distributed in the mesoporous materials.^{23,24} The pressure resistance increases substantially as the free spaces between mesoporous particles are filled with amine molecules. As a result, an amine loading at 50–75 wt% was found to be an optimal range for most mesoporous supports.^{9,23,35}

Fig. 1a–d shows TEM images for several MC x / y supports. Recall x and y correspond to the approximate diameter and the

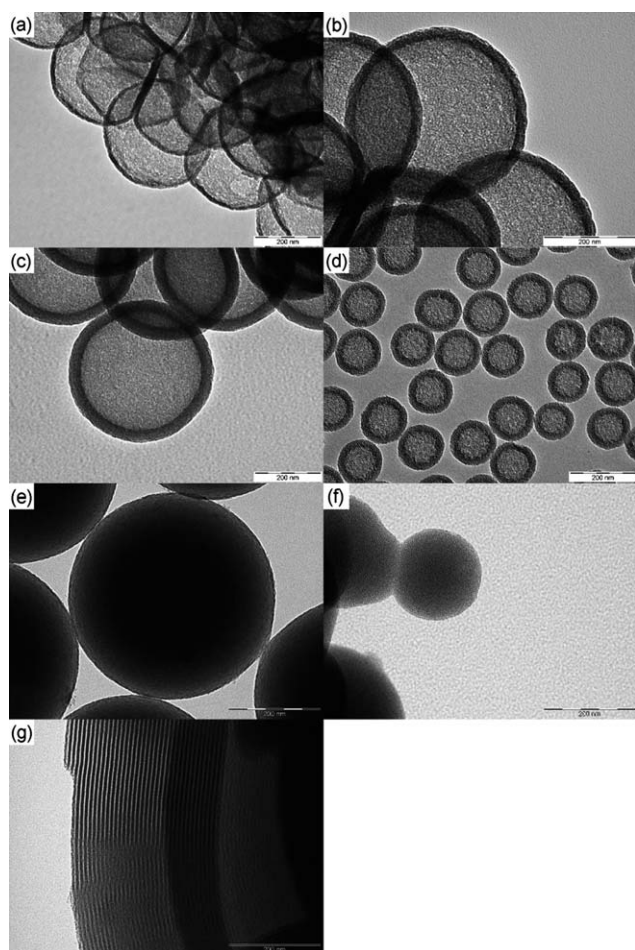


Fig. 1 Transmission electron micrographs of various silica supports. (a) MC400/10, (b) MC400/20, (c) MC400/50, (d) MC160/20, (e) silica coated polystyrene particle SiO₂-400, (f) MCM-41 and (g) SBA-15. Scale bar = 200 nm.

shell thickness of the capsules in nanometres, respectively. Uniform particles with a hollow center and a thin shell can be seen. For comparison, Fig. 1e shows solid, ~400 nm SiO₂ particles. In this case the polystyrene latex particles were coated with silica similarly to the mesoporous capsules but in the absence of structure directing agent, CTAB. Two widely used normal mesoporous supports, MCM-41 and SBA-15 solid particles, were also prepared in the absence of polystyrene template and are shown in Fig. 1f and g for comparison.

In an effort to characterize the distribution of the amine in the support the TEM characterization was extended to the composite sorbents as well. Since PEI is a viscous liquid at room temperature, half of it was substituted with the same volume of glycerol diglycidyl ether in order to prepare samples appropriate for TEM imaging. The amine–epoxy mixture was impregnated into the silica supports in the same manner as those sorbents impregnated with pure amine except that they were dried at lower temperature ~20 °C to minimize the crosslinking during the solvent removal. The polymer distribution in the sorbent was then “fixed” by crosslinking the amine–epoxy mixture at 80 °C for 6 h.

TEM images of these composites are shown in Fig. 2. In contrast to the normal mesoporous supports,^{9,11,17,23–26,35} the exceptionally large pore volume in the hollow cores of the capsules can accommodate much higher amount of amine molecules while the textured mesoporous shell can facilitate access to the interior of the capsules. As shown in Fig. 2a, the amine–epoxy polymer shows a more uniform distribution throughout the support in MC400/10PEI-GDE%83 compared with MCM-41PEI-GDE%83 (Fig. 2c). In the latter sample the support particles are submerged in a sea of amine–epoxy polymer (grey areas) even though the polymer loading is the same in both samples, suggesting that a large amount of the polymer is accommodated in the interior area of the capsules in the former. The higher magnification TEM image of MC400/10PEI-GDE%83 (Fig. 2b) further confirms the interiors of the capsules

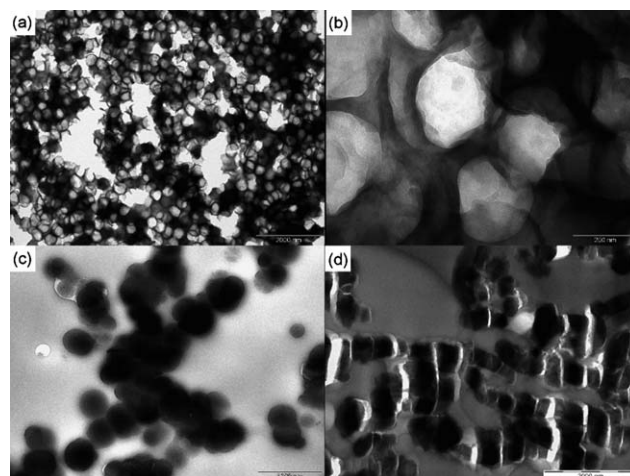


Fig. 2 Transmission electron micrographs of composites prepared by impregnation of polyethyleneimine and glycerol diglycidyl ether (v/v = 1 : 1) into the mesoporous supports. (a) MC400/10PEI-GDE%83, (b) MC400/10PEI-GDE%83 (high magnification, scale bar = 200 nm), (c) MCM-41PEI-GDE%83 and (d) SBA-15PEI-GDE%83.

are coated with the amine. The large excess of polymer outside the normal, non-hollow mesoporous particles results in sorbents that are gel-like when high loadings of amine are used (*i.e.* MCM-41PEI%83, Fig. S2b†). In contrast, sorbents based on mesoporous capsules containing the same amount of amine tend to be powders (Fig. S2a†).

Similar results are observed for SBA-15PEI-GDE%83, where a significant amount of the polymer is present outside the particles (blurry grey area, Fig. 2d) (Fig S2c†). The ability of the mesoporous capsules to accommodate uniformly higher amounts of amines is a critical feature with regard to CO₂ capture performance (*vide infra*). A higher amine loading, uniform amine distribution with less blocked pores/channels all favor more active sites available for CO₂ uptake, and therefore, a higher capacity of the sorbent.

The FT-IR spectra of composite sorbents are shown in Fig. 3. The spectra of PEI and the mesoporous silica capsules are also included for comparison. The SiO₂ capsules show a strong absorption band near 1100 cm⁻¹ due to the Si–O–Si asymmetric stretching vibrations. In the pure PEI bands at 3368, 3302 and 1595 cm⁻¹ correspond to the asymmetric and symmetric NH₂ stretching vibrations while bands at 2931, 2881, 2814, 1457 and 1346 cm⁻¹ can be due to CH₂ vibrations. As expected the composite sorbent shows peaks characteristic of both the mesoporous capsules and PEI. When the composite sorbent is exposed to CO₂ new absorption bands at 1650, 1540, and 1407 cm⁻¹ appear, which can be assigned to N–H deformation in RNH₃⁺, C=O stretch, and NCOO skeletal vibration,

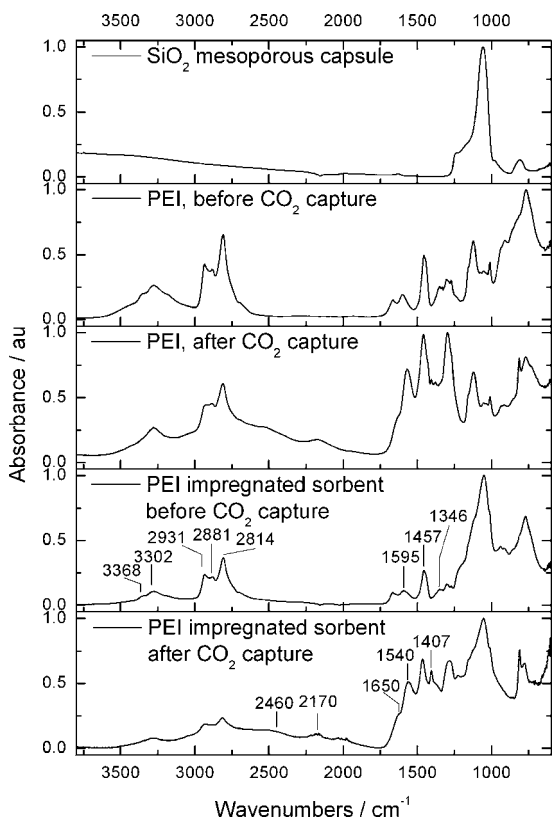


Fig. 3 FT-IR spectra of support, PEI (before and after CO₂ capture) and the nanocomposite sorbent (before and after CO₂ capture).

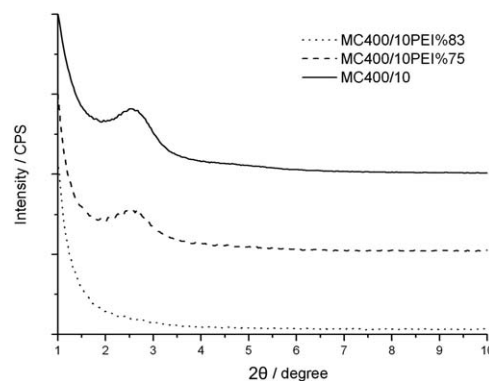


Fig. 4 XRD patterns of mesoporous silica capsules with different PEI loadings.

respectively due to the carbamate formed. The two broad bands at 2460 and 2170 cm⁻¹ after exposure to CO₂ are also the result of chemically absorbed CO₂ species.³⁶

The XRD pattern of the composite sorbents is shown in Fig. 4. The calcined MC400/10 capsules show a relatively broad diffraction peak at $2\theta = 2.55$, corresponding to a d -value of 3.45 nm. Addition of PEI into the capsules to produce MC400/10PEI%75 has little effect on their mesoporous structure, as the diffraction patterns remain virtually unchanged after the introduction of PEI. However, the intensity of the diffraction patterns does decrease especially at higher PEI loadings and in the case of MC400/10PEI%83 the diffraction peak disappears. The diffraction peak intensities can be correlated with the scattering contrast between the silicate walls and the pores. The more amine is incorporated into the pore channels, the lower the peak intensity.^{37–39} The weaker intensity of the diffraction patterns with increasing PEI loading suggests the filling of the mesoporous pores with PEI.⁹

A sample of completely degassed mesoporous capsules MC400/10 shows a surface area of 725 m² g⁻¹ and a type IV isotherm with an H3 hysteresis loop (Fig. S3†).⁴⁰ After filling the capsules with PEI (75 wt%), the surface area decreases to 19 m² g⁻¹ and a type II isotherm is seen (Fig. S3†), suggesting that access of nitrogen into the pores at liquid nitrogen temperatures is somewhat restricted. The corresponding pore volumes are 0.73 and 0.069 cm³ g⁻¹ for the empty and amine filled capsules, respectively. The surface area, pore volume and average pore diameter of all samples based on different supports and amine loadings are summarized in Table 1.

CO₂ capture kinetics

Owing to our interest in developing CO₂ sorbents several MC400/10 samples impregnated with different amounts of PEI were evaluated. As shown in Fig. 5, the CO₂ capture appears to be a two-stage process. Once the sorbents (both composites and pure amine) were in the CO₂ stream, a sharp linear weight gain occurred in the first stage, which was completed in less than 5 min followed by a second, much slower adsorption process. Similar two-stage adsorption kinetics but with a much lower first-stage capacity have been observed in other amine impregnated sorbents.^{9,14,28} It is interesting that the first stage of adsorption showed similar sorption kinetics for all our samples. However, in

Table 1 Structural features for the mesoporous supports and their composite sorbents

Sample ID	Inner diameter ^a /nm	Shell thickness ^a /nm	BET surface area ^b /m ² g ⁻¹	Pore size ^b /nm	Pore volume ^b /cm ³ g ⁻¹
MC400/10	345 ± 10	12 ± 3	7.25 × 10 ²	3.1	0.73
MC400/20	355 ± 10	24 ± 5	1.30 × 10 ³	3.1	0.48
MC400/50	350 ± 10	51 ± 5	1.32 × 10 ³	3.1	0.32
MC400/10PEI%75	345 ± 10	12 ± 3	19.48	3.0	0.069
MC400/10PEI%80	345 ± 10	12 ± 3	10.64	3.1	0.031
MC400/10PEI%83	345 ± 10	12 ± 3	6.16	3.6	0.016
MC400/20PEI%67	355 ± 10	24 ± 5	12.24	3.6	0.054
MC400/20PEI%75	355 ± 10	24 ± 5	5.53	3.6	0.011
MC400/20PEI%80 ^c	355 ± 10	24 ± 5	3.82	3.1	N/A
MC400/50PEI%67	350 ± 10	51 ± 5	9.65	3.1	0.025
MC400/50PEI%75 ^c	350 ± 10	51 ± 5	3.15	3.6	N/A
MC400/50PEI%80 ^c	350 ± 10	51 ± 5	0.45	3.6	N/A
MCM-41	N/A	N/A	1.03 × 10 ³	2.6	0.67
MCM-41PEI%75 ^c	N/A	N/A	1.80	N/A	N/A
SBA-15	N/A	N/A	8.28 × 10 ²	5.6	0.89
SBA-15PEI%75	N/A	N/A	2.38	N/A	0.023

^a Measured by TEM. ^b Measured by a nitrogen adsorption BET method. ^c The pore volume is below the detection limit.

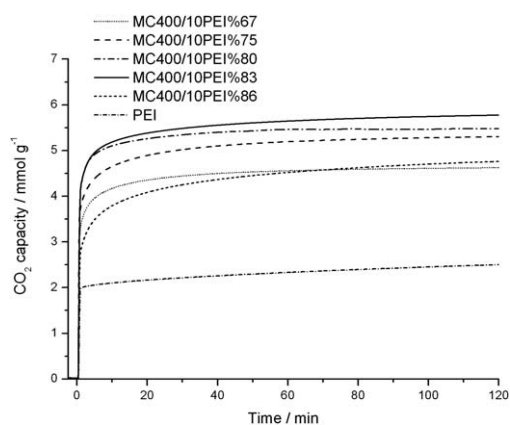


Fig. 5 CO₂ capture kinetics of mesoporous silica sorbents with different amine loadings.

the case of pure PEI the adsorption reaches a plateau quickly with a corresponding CO₂ capture capacity of about 2 mmol g⁻¹. In contrast, the composite sorbents reach a plateau at much higher values, which significantly boosts their CO₂ capacity. Note that the capture capacity of the empty capsules is virtually zero under the same CO₂ capture conditions. By increasing the amine loading from 67 to 80 wt%, the CO₂ capacity in the first stage was improved from 3.2 to 4.2 mmol g⁻¹. Increasing the amine content from 80 to 83 wt% showed no significant capacity enhancement in the first stage. Further increasing the amine loading to 86 wt%, however, resulted in a capacity drop to 2.6 mmol g⁻¹. The adsorption capacity increases somewhat during the slow second process. The adsorption kept increasing albeit at a very slow rate even after 120 min indicating that the adsorption did not reach its thermodynamic equilibrium. A capacity of up to 5.7 mmol g⁻¹ was obtained after 120 min for MC400/10PEI%83. Note that MC400/10PEI%83 reached more than 5.0 mmol g⁻¹ within the first 10 min of CO₂ exposure. The rapid kinetics are very beneficial in shortening the adsorption cycle time for potential practical applications.

The two-stage adsorption seen for all composite sorbents and pure PEI can be attributed to CO₂ diffusion resistance developed

during the process. Once the sorbent is exposed to CO₂, the fresh PEI reacts with CO₂ and yields carbamate and other CO₂-amine complexes as suggested by FT-IR spectra.^{41,42} As more CO₂ is adsorbed, the viscosity of polyethylenimine increases substantially, which builds up diffusion resistance for CO₂. In fact pure PEI becomes gel-like after CO₂ exposure (Fig. S4†). This diffusion resistance prevents PEI from achieving its theoretical thermodynamic capture capacity. Dramatic viscosity increases have been reported for other amines or ionic liquids and have been attributed to the formation of salt bridges and/or hydrogen-bonded networks of amine-CO₂ zwitterions.⁴³⁻⁴⁷ Accessibility of active sites to the CO₂ molecules due to the better distribution of the amine in the capsules reduces the diffusion resistance and contributes to the higher capacities of the composites sorbents over the pure PEI.

CO₂ capture capacity

Several types of mesoporous capsules were synthesized to evaluate the effects of the support structure on the capacity of sorbents (Fig. 6). MC160/20PEI and MC400/20PEI were compared to investigate how particle size of the support affects CO₂ capture capacity. MC160/20 and MC400/20 have a similar mesoporous shell structure and thickness but different particle sizes (Fig. 1). The maximum capacity of MC400/20PEI (5.25 mmol g⁻¹) is higher than that of MC160/20PEI (4.05 mmol g⁻¹) by 30%. The optimal amine loading (*i.e.* the amine content in the sorbent at maximum CO₂ capacity) increases from 67 wt% for MC160/20PEI to 75 wt% for MC400/20PEI. Thus, larger particle size seems to increase both the optimal amine content as well as CO₂ capture capacity.

MC400/10PEI, MC400/20PEI and MC400/50PEI were used to study the effects of shell thickness on CO₂ capacity. From Fig. 6, MC400/10PEI shows the best optimal amine loading and highest capture capacity suggesting that a thinner shell is more preferable. From Table 1 both the surface area and the pore volume of the composite sorbents decrease as the shell thickness increases. The thicker mesoporous shell layer and the smaller total pore

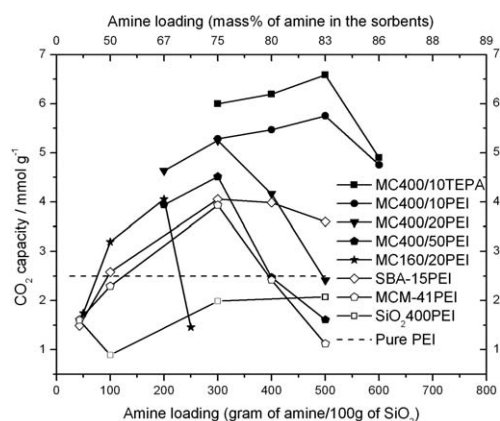


Fig. 6 CO₂ capture capacity of composite sorbents based on various mesoporous silica supports. The capture capacity was measured after 120 min at 75 °C under 1 atm pure CO₂.

volume may result in more constricted or blocked pores in the sorbents lowering capture capacity.

Most of advanced amine solid sorbents to date are based on normal mesoporous supports such as SBA-15 and MCM-41.^{9,28} Therefore, several sorbents using these supports were prepared to compare under identical conditions with the composite sorbents based on the mesoporous capsules. The CO₂ capacity of these sorbents with various amine loadings was measured under 1 atm CO₂ at 75 °C and the results are included in Fig. 6. The SBA-15 based sorbents show a moderately higher capacity than those based on MCM-41 at the same amine loading. Both the SBA-15 and MCM-41 based sorbents show an optimal amine loading at 75 wt% and a capacity around 4 mmol g⁻¹. MC400/10PEI%83 has a capacity enhancement by at least 40% over the sorbents based on these normal mesoporous supports, suggesting that the mesoporous capsules are more advantageous over other porous materials used as support. Under the testing conditions, the stoichiometry of CO₂ and amine (CO₂/N) for MC400/10PEI%75 and MC400/10PEI%83 is around 0.3, which, although still lower than the theoretical stoichiometry of 0.5,¹⁴ is much higher than those of MCM-41PEI%75 (CO₂/N = 0.22) and SBA-15PEI%75 (CO₂/N = 0.23). For complete comparison we have prepared and evaluated composite sorbents based on “solid” SiO₂ coated particles of similar size as the capsules (*i.e.* particles prepared in the absence of a structure directing agent and without removing the PS latex, Fig. 1e). The sorbent based on the nonporous nanoparticles, SiO₂-400PEI, has poor capacity even lower than that of pure PEI despite that the size of the support is similar to that of MC400/10.

Other than the structure of the support, the effect of amine type on the adsorption capacity was investigated using two different amines, PEI and TEPA. As shown in Fig. 6, the optimal amine loading was not affected by the type of amine and both were about 83 wt%. However, a higher CO₂ capacity was obtained from MC400/10TEPA than MC400/10PEI at the same amine loading and the stoichiometry of CO₂ and amine (CO₂/N) was improved to 0.33. We suspect that the higher density of amino groups and less viscous nature of TEPA compared to PEI provide more reactive sites for CO₂ and thus a higher overall adsorption capacity.

Table 2 Capture capacity of composite sorbents at low CO₂ partial pressure at 75 °C

Sample ID	CO ₂ concentration (%)	Sorbent capacity/mmol g ⁻¹
MC400/10PEI%83	20.0	4.91
MC400/10PEI%83	10.0	4.45
MC400/10PEI%83 ^a	10.0	5.58
MC400/10TEPA%83	20.0	6.39
MC400/10TEPA%83	10.0	5.57
MC400/10TEPA%83 ^a	10.0	7.93

^a The test gas was pre-humidified to a steady state by flowing through two glass water bubblers at room temperature.

The performance of the composite sorbents, MC400/10PEI%83 and MC400/10TEPA%83, in a low CO₂ concentration dry gas (balanced with N₂ or Ar) and simulated flue gas was also investigated and the results are summarized in Table 2. The two sorbents exhibit outstanding capacities above 4.4 mmol g⁻¹ even at 0.1 atm dry CO₂. When simulated flue gas (pre-humidified 10% CO₂) was used, the capacity of MC400/10PEI%83 increased to 5.58 mmol g⁻¹ and that of MC400/10TEPA%83 to 7.93 mmol g⁻¹. The positive effect of moisture on the capacity of amine functionalized sorbents has been reported before.^{17,19,27,48} It was claimed that the formation of bicarbonate in the presence of moisture contributes to the increase of the capacity.^{17,19,27,48}

Cyclic adsorption–desorption studies

For potential practical applications, in addition to high CO₂ capturing capacity, the sorbent must possess long-term stability and regenerability with a minimum difference in adsorption/desorption temperatures or pressures to lower cost. At the same time, a short cycle time is generally preferred. To this end, two processes, temperature swing and concentration sweep, were used to evaluate the stability and regenerability of the mesoporous capsule sorbents in a short cycling time. Fig. 7 depicts the adsorption–desorption cycles of MC400/10PEI%83 and MC400/10TEPA%83 using a temperature swing process. After exposure to dry CO₂ at 75 °C for 10 min, the temperature was increased to

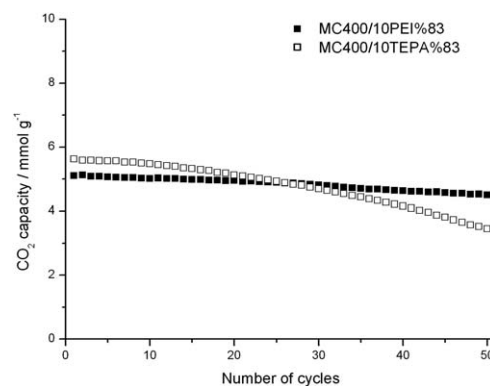


Fig. 7 Cyclic adsorption–desorption of sorbents based on mesoporous silica capsules containing 83% amine using a temperature swing (CO₂ capture at 75 °C under 1 atm pure CO₂ for 10 min; sorbent desorption at 100 °C under 1 atm pure N₂ for 10 min).

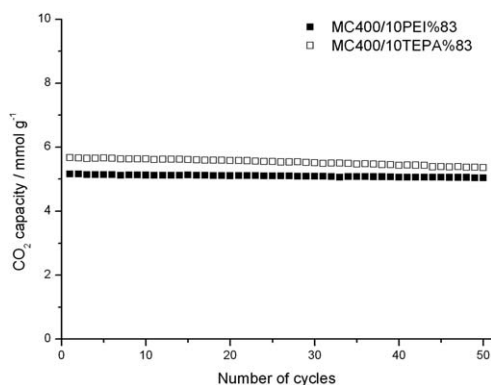


Fig. 8 Cyclic adsorption–desorption of sorbents based on mesoporous silica capsules containing 83% amine using a concentration sweep (CO_2 capture at 75°C under 1 atm pure CO_2 for 10 min; sorbent desorption at 75°C under 1 atm pure N_2 for 25 min).

100°C . Both sorbents can be regenerated within 10 min in N_2 . MC400/10PEI%83 was more stable than MC400/10TEPA%83. The former retained $\sim 88\%$ of its capacity whereas MC400/10TEPA%83 dropped to about 60% of its capacity after 50 cycles. The better cyclic performance of MC400/10PEI%83 may be due to the higher boiling point of PEI, which contributes to better temperature stability. Fig. 8 shows the regeneration behavior of MC400/10PEI%83 and MC400/10TEPA%83 using a concentration sweep process. After CO_2 capture at 75°C , N_2 was used as the stripping gas to remove the CO_2 from the sorbent at the same temperature for 25 min. Both MC400/10PEI%83 and MC400/10TEPA%83 had only a slight decrease in capacity (less than 10%) after 50 cycles.

Conclusion

We have synthesized and evaluated a new, highly efficient CO_2 sorbent platform based on specially designed mesoporous silica capsules impregnated with polyethylenimine (PEI) and tetraethylenepentamine (TEPA). The specially designed capsules offer increased amount of amine incorporation and reactive sites for CO_2 capture leading to exceptional capturing performance of up to 7.93 mmol g^{-1} in simulated flue gas. In addition to the simple synthesis and their outstanding CO_2 capture capacity, the sorbents are readily and fully regenerated at relatively low temperature ($<100^\circ\text{C}$) and exhibit good stability over repetitive adsorption–desorption cycling.

Acknowledgements

This publication was based on work supported by award no. KUS-C1-018-02, made by King Abdullah University of Science and Technology (KAUST).

References

- 1 P. M. Cox, R. A. Betts, C. D. Jones, S. A. Spall and I. J. Totterdell, *Nature*, 2000, **408**, 184–187.
- 2 F. Y. Jou, A. E. Mather and F. D. Otto, *Can. J. Chem. Eng.*, 1995, **73**, 140–147.
- 3 H. L. Bai and A. C. Yeh, *Ind. Eng. Chem. Res.*, 1997, **36**, 2490–2493.
- 4 S. Bishnoi and G. T. Rochelle, *Chem. Eng. Sci.*, 2000, **55**, 5531–5543.

- 5 G. Puxty, R. Rowland, A. Allport, Q. Yang, M. Bown, R. Burns, M. Maeder and M. Attalla, *Environ. Sci. Technol.*, 2009, **43**, 6427–6433.
- 6 N. Zhang and N. Lior, *Energy*, 2006, **31**, 1666–1679.
- 7 R. Bredesena, K. Jordal and A. Bolland, *Chem. Eng. Process.*, 2004, **43**, 1129–1158.
- 8 C. E. Powell and G. G. Qiao, *J. Membr. Sci.*, 2006, **279**, 1–49.
- 9 X. C. Xu, C. S. Song, J. M. Andresen, B. G. Miller and A. W. Scaroni, *Energy Fuels*, 2002, **16**, 1463–1469.
- 10 J. C. Abanades, *Chem. Eng. J.*, 2002, **90**, 303–306.
- 11 J. C. Hicks, J. H. Drese, D. J. Fauth, M. L. Gray, G. G. Qi and C. W. Jones, *J. Am. Chem. Soc.*, 2008, **130**, 2902–2903.
- 12 A. B. Rao and E. S. Rubin, *Environ. Sci. Technol.*, 2002, **36**, 4467–4475.
- 13 D. Bonenfant, M. Mimeault and R. Hausler, *Ind. Eng. Chem. Res.*, 2003, **42**, 3179–3184.
- 14 S. Choi, J. H. Drese and C. W. Jones, *ChemSusChem*, 2009, **2**, 796–854.
- 15 M. Radosz, X. D. Hu, K. Krutkramelis and Y. Q. Shen, *Ind. Eng. Chem. Res.*, 2008, **47**, 3783–3794.
- 16 M. L. Gray, Y. Soong, K. J. Champagne, H. Pennline, J. P. Baltrus, R. W. Stevens, R. Khatri, S. S. C. Chuang and T. Filburn, *Fuel Process. Technol.*, 2005, **86**, 1449–1455.
- 17 G. Knowles, J. Graham, S. Delaney and A. Chaffee, *Fuel Process. Technol.*, 2005, **86**, 1435–1448.
- 18 A. Sayari and Y. Belmabkhout, *J. Am. Chem. Soc.*, 2010, **132**, 6312–6314.
- 19 X. C. Xu, C. S. Song, B. G. Miller and A. W. Scaroni, *Ind. Eng. Chem. Res.*, 2005, **44**, 8113–8119.
- 20 X. C. Xu, C. S. Song, J. M. Andresen, B. G. Miller and A. W. Scaroni, *Microporous Mesoporous Mater.*, 2003, **62**, 29–45.
- 21 C. S. Song, X. C. Xu, J. M. Andresen, B. G. Miller and A. W. Scaroni, *Stud. Surf. Sci. Catal.*, 2004, **153**, 411–416.
- 22 F. Zheng, D. N. Tran, B. J. Busche, G. E. Fryxell, R. S. Addleman, T. S. Zemanian and C. L. Aardahl, *Ind. Eng. Chem. Res.*, 2005, **44**, 3099–3105.
- 23 M. B. Yue, L. B. Sun, Y. Cao, Y. Wang, Z. J. Wang and J. H. Zhu, *Chem.–Eur. J.*, 2008, **14**, 3442–3451.
- 24 M. B. Yue, Y. Chun, Y. Cao, X. Dong and J. H. Zhu, *Adv. Funct. Mater.*, 2006, **16**, 1717–1722.
- 25 G. P. Knowles, S. W. Delaney and A. L. Chaffee, *Ind. Eng. Chem. Res.*, 2006, **45**, 2626–2633.
- 26 P. J. E. Harlick and A. Sayari, *Ind. Eng. Chem. Res.*, 2006, **45**, 3248–3255.
- 27 C. Chen, S. T. Yang, W. S. Ahn and R. Ryoo, *Chem. Commun.*, 2009, 3627–3629.
- 28 X. L. Ma, X. X. Wang and C. S. Song, *J. Am. Chem. Soc.*, 2009, **131**, 5777–5783.
- 29 J. Drese, S. Choi, R. Lively, W. Koros, D. Fauth, M. Gray and C. Jones, *Adv. Funct. Mater.*, 2009, **19**, 3821–3832.
- 30 G. F. Schuette, E. G. Latimer, J. B. Cross and E. Esen, *Fifth Annual Conference on Carbon Capture and Sequestration*, Alexandria, Virginia, 2006.
- 31 G. Qi, Y. Wang, L. Estevez, A. Switzer, X. Duan, Y. Yang and E. P. Giannelis, *Chem. Mater.*, 2010, **22**, 2693–2695.
- 32 D. Y. Zhao, J. L. Feng, Q. S. Huo, N. Melosh, G. H. Fredrickson, B. F. Chmelka and G. D. Stucky, *Science*, 1998, **279**, 548–552.
- 33 O. Leal, C. Bolivar, C. Ovalles, J. J. Garcia and Y. Espidel, *Inorg. Chim. Acta*, 1995, **240**, 183–189.
- 34 H. Y. Huang, R. T. Yang, D. Chinn and C. L. Munson, *Ind. Eng. Chem. Res.*, 2003, **42**, 2427–2433.
- 35 W. J. Son, J. S. Choi and W. S. Ahn, *Microporous Mesoporous Mater.*, 2008, **113**, 31–40.
- 36 X. X. Wang, V. Schwartz, J. C. Clark, X. L. Ma, S. H. Overbury, X. C. Xu and C. S. Song, *J. Phys. Chem. C*, 2009, **113**, 7260–7268.
- 37 B. Marler, U. Oberhagemann, S. Vortmann and H. Gies, *Microporous Mater.*, 1996, **6**, 375–383.
- 38 W. Hammond, E. Prouzet, S. D. Mahanti and T. J. Pinnavaia, *Microporous Mesoporous Mater.*, 1999, **27**, 19–25.
- 39 J. Sauer, F. Marlow and F. Schuth, *Phys. Chem. Chem. Phys.*, 2001, **3**, 5579–5584.
- 40 K. S. W. Sing, D. H. Everett, R. A. W. Haul, L. Moscou, R. A. Pierotti, J. Rouquerol and T. Siemieniowska, *Pure Appl. Chem.*, 1985, **57**, 603–619.
- 41 F. Goodridge, *Trans. Faraday Soc.*, 1955, **51**, 1703–1709.

- 42 S. Satyapal, T. Filburn, J. Trela and J. Strange, *Energy Fuels*, 2001, **15**, 250–255.
- 43 P. V. Danckwerts, *Chem. Eng. Sci.*, 1979, **34**, 443–446.
- 44 M. Caplow, *J. Am. Chem. Soc.*, 1968, **90**, 6795–6803.
- 45 T. G. Amundsen, L. E. Oi and D. A. Eimer, *J. Chem. Eng. Data*, 2009, **54**, 3096–3100.
- 46 M. D. Soutullo, C. I. Odom, B. F. Wicker, C. N. Henderson, A. C. Stenson and J. H. Davis, *Chem. Mater.*, 2007, **19**, 3581–3583.
- 47 K. E. Gutowski and E. J. Maginn, *J. Am. Chem. Soc.*, 2008, **130**, 14690–14704.
- 48 X. C. Xu, C. S. Song, B. G. Miller and A. W. Scaroni, *Fuel Process. Technol.*, 2005, **86**, 1457–1472.